Iowa State University

From the SelectedWorks of Song Zhang

August 21, 2006

Novel method for structured light system calibration

Song Zhang, *Harvard University*
Peisen S. Huang, *State University of New York at Stony Brook*

Available at: http://works.bepress.com/song_zhang/31/

SELECTEDWORKS™

Novel method for structured light system calibration

Song Zhang, MEMBER SPIE
Harvard University
Mathematics Department
Cambridge, Massachusetts 02138
E-mail: szhang@fas.harvard.edu

Peisen S. Huang, MEMBER SPIE
State University of New York at Stony Brook
Department of Mechanical Engineering
Stony Brook, New York 11794
E-mail: peisen.huang@stonybrook.edu

Abstract. System calibration, which usually involves complicated and time-consuming procedures, is crucial for any 3-D shape measurement system. In this work, a novel systematic method is proposed for accurate and quick calibration of a 3-D shape measurement system we developed based on a structured light technique. The key concept is to enable the projector to "capture" images like a camera, thus making the calibration of a projector the same as that of a camera. With this new concept, the calibration of structured light systems becomes essentially the same as the calibration of traditional stereovision systems, which is well established. The calibration method is fast, robust, and accurate. It significantly simplifies the calibration and recalibration procedures of structured light systems. This work describes the principle of the proposed method and presents some experimental results that demonstrate its performance. *© 2006 Society of Photo-Optical Instrumentation Engineers.*
[DOI: 10.1117/1.2336196]

Subject terms: 3-D shape measurement; calibration; structured light system; projector image; phase shifting.

Paper 050866 received Oct. 31, 2005; accepted for publication Jan. 9, 2006; published online Aug. 21, 2006.

1 Introduction

Accurate measurement of the 3-D shape of objects is a rapidly expanding field, with applications in entertainment, design, and manufacturing. Among the existing 3-D shape measurement techniques, structured-light-based techniques are increasingly used due to their fast speed and noncontact nature. A structured light system differs from a classic stereo vision system in that it avoids the fundamentally difficult problem of stereo matching by replacing one camera with a light pattern projector. The key to accurate reconstruction of the 3-D shape is the proper calibration of each element used in the structured light system.[1] Methods based on neural networks,[2,3] bundle adjustment,[4–9] or absolute phase[10] have been developed, in which the calibration process varies depending on the available system parameters information and the system setup. It usually involves complicated and time-consuming procedures.

In this research, a novel approach is proposed for accurate and quick calibration of the structured light system we developed. In particular, a new method is developed that enables a projector to "capture" images like a camera, thus making the calibration of a projector the same as that of a camera, which is well established. Project calibration is highly important because today, projectors are increasingly used in various measurement systems, yet so far no systematic way of calibrating them has been developed. With this new method, the projector and the camera can be calibrated independently, which avoids the problems related to the coupling of the errors of the camera and the projector. By treating the projector as a camera, we essentially unified the calibration procedures of a structured light system and a classic stereo vision system. For the system developed in this research, a linear model with a small look-up Table (LUT) for error compensation is found to be sufficient.

The rest of the work is organized as follows. Section 2 introduces the principle of the proposed calibration method. Section 3 shows some experimental results. Section 4 evaluates the calibration results. Section 5 discusses the advantages and disadvantages of this calibration method. Finally, Sec. 6 concludes the work.

2 Principle

2.1 *Camera Model*

Camera calibration has been extensively studied over the years. A camera is often described by a pinhole model, with intrinsic parameters including focal length, principle point, pixel skew factor, and pixel size; and extrinsic parameters including rotation and translation from a world coordinate system to a camera coordinate system. Figure 1 shows a typical diagram of a pinhole camera model, where p is an arbitrary point with coordinates (x^w, y^w, z^w) and (x^c, y^c, z^c) in the world coordinate system $\{o^w; x^w, y^w, z^w\}$ and camera coordinate system $\{o^c; x^c, y^c, z^c\}$, respectively. The coordinate of its projection in the image plane $\{o; u, v\}$ is (u, v). The relationship between a point on the object and its projection on the image sensor can be described as follows based on a projective model:

$$sI = A[R, t]X^w, \tag{1}$$

where $I = \{u, v, 1\}^T$ is the homogeneous coordinate of the image point in the image coordinate system, $X^w = \{x^w, y^w, z^w, 1\}^T$ is the homogeneous coordinate of the point in the world coordinate system, and s is a scale factor.

0091-3286/2006/$22.00 © 2006 SPIE

Downloaded From: http://opticalengineering.spiedigitallibrary.org/ on 11/05/2014 Terms of Use: http://spiedl.org/terms

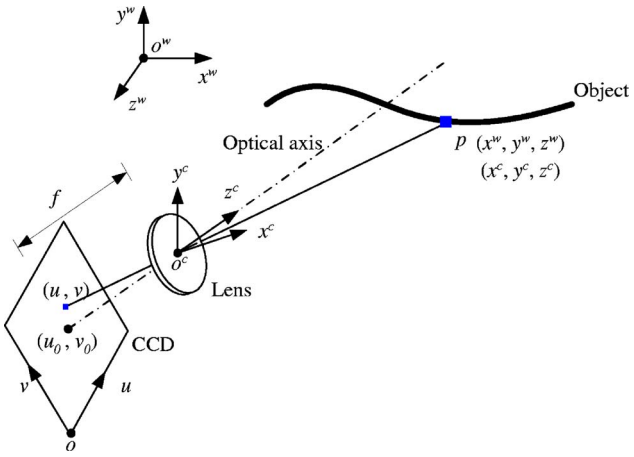

Fig. 1 Pinhole camera model.

$[R,t]$, called an extrinsic parameters matrix, represents rotation and translation between the world coordinate system and camera coordinate system. A is the camera intrinsic parameters matrix and can be expressed as

$$A = \begin{bmatrix} \alpha & \gamma & u_0 \\ 0 & \beta & v_0 \\ 0 & 0 & 1 \end{bmatrix},$$

where (u_0, v_0) is the coordinate of principle point, α and β are focal lengths along the u and v axes of the image plane, and γ is the parameter that describes the skewness of two image axes. Equation (1) represents the linear model of the camera. More elaborate nonlinear models are discussed in Refs. 11–14. In this research, a linear model is found to be sufficient to describe our system.

2.2 *Camera Calibration*

To obtain intrinsic parameters of the camera, a flat checkerboard is usually used. In this research, instead of a standard black-and-white (B/W) checkerboard, we use a red/blue checkerboard with a checker size of 15×15 mm, as shown in Fig. 2. The reason of using such a colored checkerboard is explained in detail in Sec. 2.3. The calibration procedures follow Zhang's method.[15] The flat checkerboards positioned with different poses are imaged by the camera. A total of ten images, as shown in Fig. 3, are used to obtain intrinsic parameters of the camera using the Matlab toolbox provided by Bouguet.[16] The intrinsic parameters matrix based on the linear model is obtained as

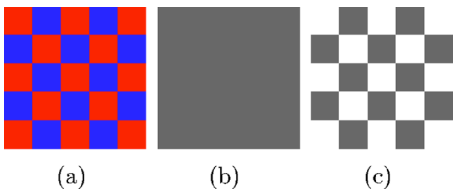

Fig. 2 Checkerboard for calibration: (a) red/blue checkerboard, (b) B/W image with white light illumination, and (c) B/W image with red light illumination (Color online only).

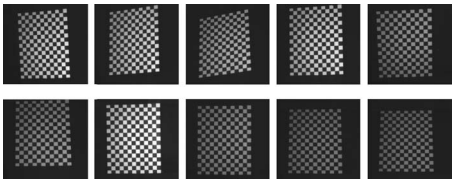

Fig. 3 Checkerboard images for camera calibration.

$$A^c = \begin{bmatrix} 25.8031 & 0 & 2.7962 \\ 0 & 25.7786 & 2.4586 \\ 0 & 0 & 1 \end{bmatrix} \text{mm},$$

for our camera (Dalsa CA-D6-0512) with a 25-mm lens (Fujinon HF25HA-1B). The size of each charge-coupled device (CCD) pixel is 10×10-μm square and the total number of pixels is 532×500. We found that the principle point deviated from the CCD center, which might have been caused by misalignment during the camera assembling process.

2.3 *Projector Calibration*

A projector can be regarded as the inverse of a camera, because it projects images instead of capturing them. In this research, we propose a method that enables a projector to "capture" images like a camera, thus making the calibration of a projector essentially the same as that of a camera, which is well established.

2.3.1 *Digital micromirror device image generation*

If a projector can capture images like a camera, its calibration will be as simple as the calibration of a camera. However, a projector obviously cannot capture images directly. In this research, we propose a new concept of using a camera to capture images "for" the projector and then transforming the images into projector images, so that they are as if captured directly by the projection chip (digital micromirror device or DMD) in the projector. The key to realizing this concept is to establish the correspondence between camera pixels and projector pixels.

In this research, we use a phase-shifting method to accomplish this task. The phase-shifting method is also the method used in our structured light system for 3-D shape measurement. In this method, three sinusoidal phase-shifted fringe patterns are generated in a computer and projected to the object sequentially by a projector. These patterns are then captured by a camera. Based on a phase-shifting algorithm, the phase at each pixel can be calculated, which is between 0 and 2π. If there is only one sinusoidal fringe in the fringe patterns, then the phase value at each camera pixel can be used to find a line of corresponding pixels on the DMD. If vertical fringe patterns are used, this line is a vertical line. If horizontal fringe patterns are used, then this line is a horizontal line. If both vertical and horizontal fringe patterns are used, then the pixel at the intersection of these two lines is the corresponding pixel of the camera pixel on the DMD. Since the use of a single fringe limits phase measurement accuracy, fringe patterns with multiple fringes are usually used. When multiple fringes are used, the phase-shifting algorithm provides only a relative phase

Downloaded From: http://opticalengineering.spiedigitallibrary.org/ on 11/05/2014 Terms of Use: http://spiedl.org/terms

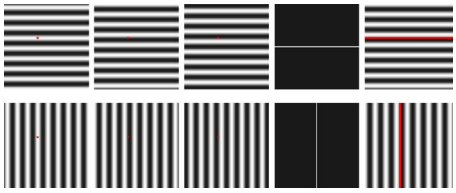

Fig. 4 Correspondence between the CCD image and the DMD image. Images in the first row from left to right are horizontal CCD fringe images I_1(−120 deg), I_2(0 deg), and I_3(120 deg), CCD centerline image, and DMD fringe image. The second row shows the corresponding images for vertical fringe images.

value. To determine the correspondence, the absolute phase value is required. In this research, we use an additional centerline image to determine absolute phase at each pixel. The following paragraph explains the details of this method.

Figure 4 illustrates how the correspondence between the CCD pixels and the DMD pixels is established. The red point shown in the upper left three fringe images is an arbitrary pixel whose absolute phase value needs to be determined. Here, absolute phase value means the phase value of the corresponding pixel on the DMD. The upper left three images are the horizontal fringe images captured by a camera. Their intensities are

$$I_1(x,y) = I'(x,y) + I''(x,y)\cos[\phi(x,y) - 2\pi/3], \tag{2}$$

$$I_2(x,y) = I'(x,y) + I''(x,y)\cos[\phi(x,y)], \tag{3}$$

$$I_3(x,y) = I'(x,y) + I''(x,y)\cos[\phi(x,y) + 2\pi/3], \tag{4}$$

where $I'(x,y)$ is the average intensity, $I''(x,y)$ is the intensity modulation, and $\phi(x,y)$ is the phase to be determined. Solving these three equations simultaneously, we obtain

$$\phi(x,y) = \arctan[\sqrt{3}(I_1 - I_3)/(2I_2 - I_1 - I_3)]. \tag{5}$$

This equation provides the so-called modulo 2π phase at each pixel, whose values range from 0 to 2π. If there is only one fringe in the projected pattern, this phase is the absolute phase. However, if there are multiple fringes in the projected pattern, 2π discontinuity is generated, the removal of which requires the use of a so-called phase unwrapping algorithm.[17]

The phase value so obtained is relative and does not represent the true phase value of the corresponding pixel on the DMD, or the absolute phase. To obtain the absolute

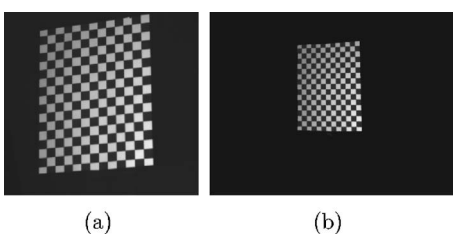

(a) (b)

Fig. 5 CCD image and its corresponding DMD image: (a) CCD image and (b) DMD image.

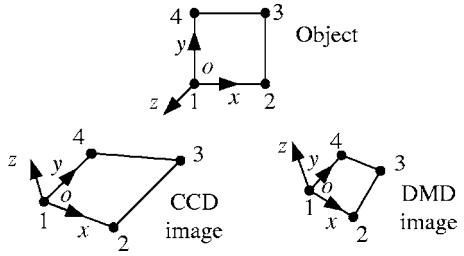

Fig. 6 World coordinate system.

phase value at each pixel, additional information is needed. In this research, we use an additional centerline image (see the fourth image on the upper row of Fig. 4) to convert the relative phase map to its corresponding absolute phase map. The bright line in this centerline image corresponds to the centerline on the DMD, where the absolute phase value is assumed to be zero. By identifying the pixels along this centerline, we can calculate the average phase of these pixels in the relative phase map as follows:

$$\bar{\phi}_0 = \frac{\sum_{n=0}^{N} \phi_n(i,j)}{N}, \tag{6}$$

where N is the number of pixels on the centerline. Obviously at these pixels, the absolute phase value should be zero. Therefore, we can convert the relative phase map into its corresponding absolute phase map by simply shifting the relative phase map by $\bar{\phi}_0$. That is,

$$\phi_a(i,j) = \phi(i,j) - \bar{\phi}_0. \tag{7}$$

After the absolute phase map is obtained, a unique point-to-line mapping between the CCD pixels and DMD pixels can be established.

Once the absolute phase value at the pixel marked in red in the upper left three images is determined, a corresponding horizontal line in the DMD image, shown in red in the last image of the upper row in Fig. 4, can be identified. This is a one-too-many mapping. If similar steps are applied to the fringe images with vertical fringes, as shown on the lower row of images in Fig. 3, another one-too-many mapping can be established. The same point on the CCD images is mapped to a vertical line in the DMD image, which is shown in red in the last image of the lower row of images in Fig. 4. The intersection point of the horizontal line and the vertical line is the corresponding point on the DMD of the arbitrary point on the CCD. Therefore, by using this

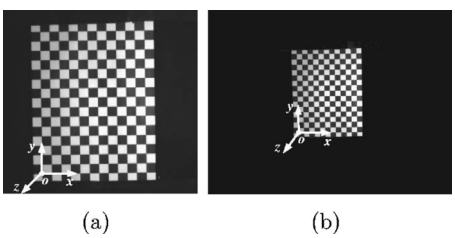

(a) (b)

Fig. 7 World coordinate system construction: (a) CCD image and (b) DMD image.

Downloaded From: http://opticalengineering.spiedigitallibrary.org/ on 11/05/2014 Terms of Use: http://spiedl.org/terms

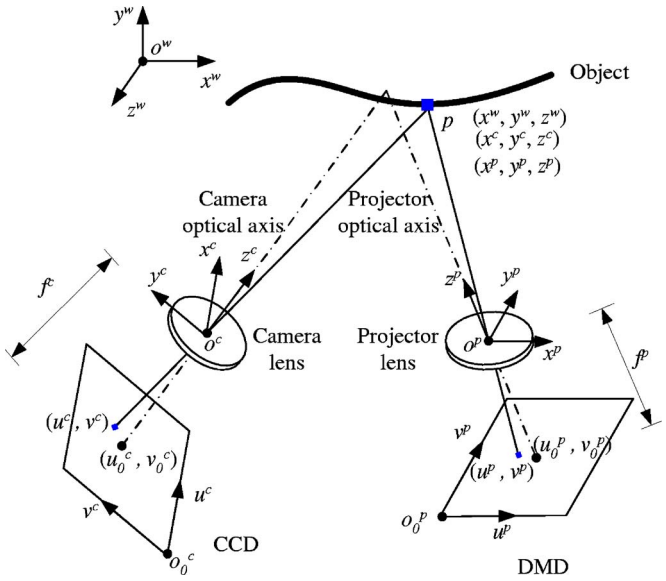

Fig. 8 Structured light system configuration.

method, we can establish a one-to-one mapping between a CCD image and a DMD image. In other words, a CCD image can be transformed to the DMD pixel by pixel to form an image, which is called the DMD image and is regarded as the image "captured" by the projector.

For camera calibration, a standard B/W checkerboard is usually used. However, in this research, a B/W checkerboard cannot be used, since the fringe images captured by the camera do not have enough contrast in the areas of the black squares. To avoid this problem, a red/blue checkerboard, illustrated in Fig. 2(a) is utilized. Because the responses of the B/W camera to red and blue colors are similar, the B/W camera can only see a uniform board (in the ideal case) if the checkerboard is illuminated by white light, as illustrated in Fig. 2(b). When the checkerboard is illuminated by red or blue light, the B/W camera will see a regular checkerboard. Figure 2(c) shows the image of the checkerboard with red light illumination. This checkerboard image can be mapped onto the DMD chip to form its corresponding DMD image for projector calibration.

In summary, the projector captures the checkerboard images through the following steps.

1. Capture three B/W phase-shifted horizontal fringe images and a horizontal centerline image projected by the projector with B/W light illumination.
2. Capture three B/W phase-shifted vertical fringe images and vertical centerline images projected by the projector with B/W light illumination.
3. Capture the image of the checkerboard with red light illumination.
4. Determine the one-to-one pixel-wise mapping between the CCD and DMD.
5. Map the image of the checkerboard with red light illumination to the DMD to create the corresponding DMD image.

Figure 5 shows an example of converting a CCD checkerboard image to its corresponding DMD image. Figure 5(a) shows the checkerboard image captured by the camera with red light illumination, while Fig. 5(b) shows the corresponding DMD image. One can verify the accuracy of the DMD image by projecting it onto the real checkerboard and checking its alignment. If the alignment is good, it means that the DMD image created is accurate.

2.3.2 *Projector calibration*

After a set of DMD images is generated, the calibration of intrinsic parameters of a projector can follow that of a camera. The following matrix,

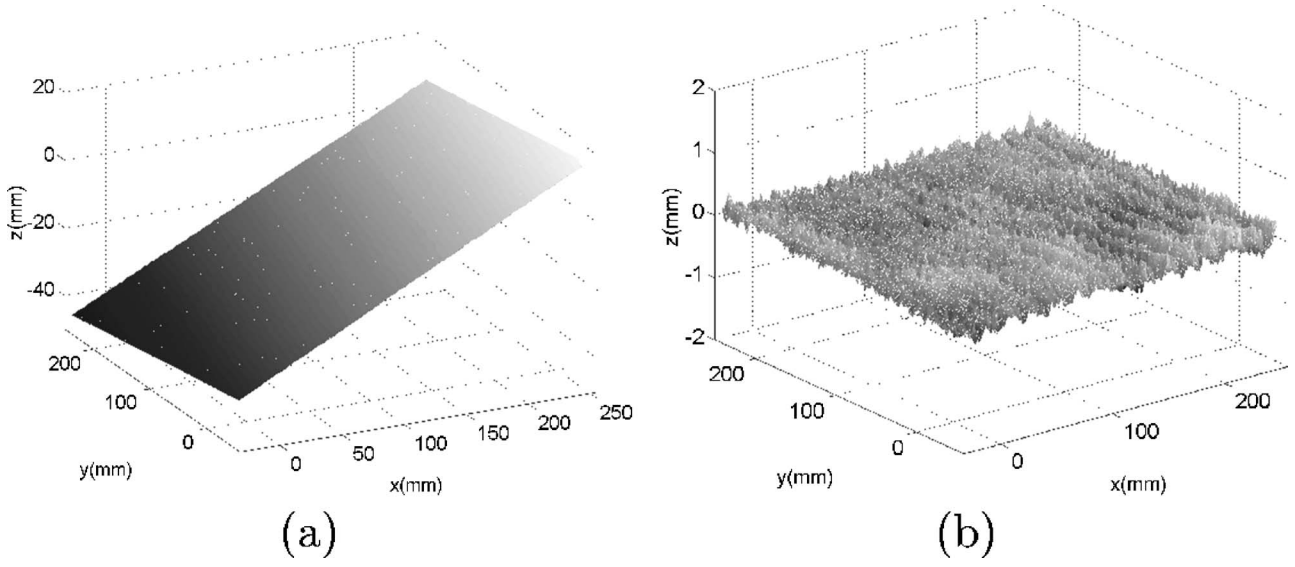

Fig. 9 3-D measurement result of a planar surface: (a) 3-D plot of the measured plane and (b) measurement error (rms: 0.12 mm).

Downloaded From: http://opticalengineering.spiedigitallibrary.org/ on 11/05/2014 Terms of Use: http://spiedl.org/terms

Fig. 10 3-D measurement result of sculpture Zeus.

$$A^p = \begin{bmatrix} 31.1384 & 0 & 6.7586 \\ 0 & 31.1918 & -0.1806 \\ 0 & 0 & 1 \end{bmatrix},$$

is the intrinsic parameter matrix obtained for our projector (Plus U2-1200). The DMD has a resolution of 1024×768 pixels. Its micromirror size is 13.6×13.6 μm square. We notice that the principle point deviates from the nominal center significantly in one direction, even outside the DMD chip. This is due to the fact that the projector is designed to project images along an off-axis direction.

2.4 *System Calibration*

After intrinsic parameters of the camera and the projector are calibrated, the next task is to calibrate the extrinsic parameters of the system. For this purpose, a unique world coordinate system for the camera and projector has to be established. In this research, a world coordinate system is established based on one calibration image set with its xy axes on the plane, and z axis perpendicular to the plane and pointing toward the system.

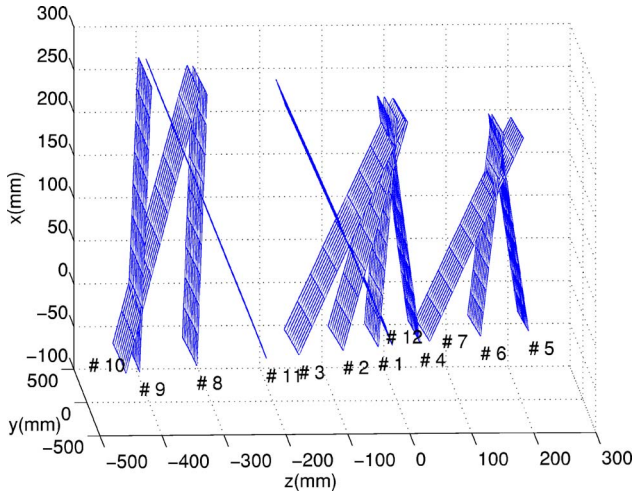

Fig. 11 Positions and orientations of the planar board for calibration evaluation.

Figure 6 shows a checker square on the checkerboard and its corresponding CCD and DMD images. The four corners 1, 2, 3, 4 of this square are imaged onto the CCD and DMD, respectively. We chose corner 1 as the origin of the world coordinate system, the direction from 1 to 2 as the x positive direction, and the direction from 1 to 4 as the y positive direction. The z axis is defined based on the right-hand rule in Euclidean space. In this way, we can define the same world coordinate system based on CCD and DMD images. Figure 7 illustrates the origin and the directions of the x, y, and z axes on these images.

Table 1 Measurement data of the testing plane at different positions and orientations.

Plane	Normal	x range (mm)	y range (mm)	z range (mm)	rms error (mm)
1	(−0.1189, 0.0334, 0.9923)	[−32.55, 236.50]	[−58.60, 238.81]	[−43.47, −1.47]	0.10
2	(−0.3660, 0.0399, 0.9297)	[−36.05, 234.77]	[−64.24, 243.10]	[−102.24, 14.61]	0.10
3	(−0.5399, 0.0351, 0.8410)	[−40.46, 234.93]	[−72.86, 248.25]	[−172.84, 11.61]	0.13
4	(0.1835, 0.0243, 0.9827)	[−60.11, 233.74]	[−60.11, 233.74]	[−22.37, 33.31]	0.10
5	(0.1981, 0.0259, 0.9798)	[−17.52, 217.04]	[−38.04, 221.09]	[156.22, 209.44]	0.11
6	(−0.1621, 0.0378, 0.9860)	[−22.33, 216.39]	[−37.42, 226.71]	[122.37, 171.38]	0.11
7	(−0.5429, 0.0423, 0.8387)	[−27.41, 212.85]	[−47.36, 232.86]	[38.06, 202.34]	0.10
8	(−0.0508, 0.0244, 0.9984)	[−50.66, 272.30]	[−96.88, 260.18]	[−336.22, −310.53]	0.22
9	(−0.0555, 0.0149, 0.9983)	[−56.38, 282.45]	[−108.03, 266.72]	[−425.85, −400.54]	0.22
10	(−0.3442, 0.0202, 0.9387)	[−57.74, 273.35]	[−106.63, 268.37]	[−448.48, −322.44]	0.22
11	(0.4855, −0.0000, 0.8742)	[−43.70, 281.07]	[−106.88, 260.01]	[−394.84, −214.85]	0.20
12	(0.5217, −0.0037, 0.8531)	[−31.12, 256.75]	[−81.14, 245.23]	[−185.51, −10.41]	0.16

Downloaded From: http://opticalengineering.spiedigitallibrary.org/ on 11/05/2014 Terms of Use: http://spiedl.org/terms

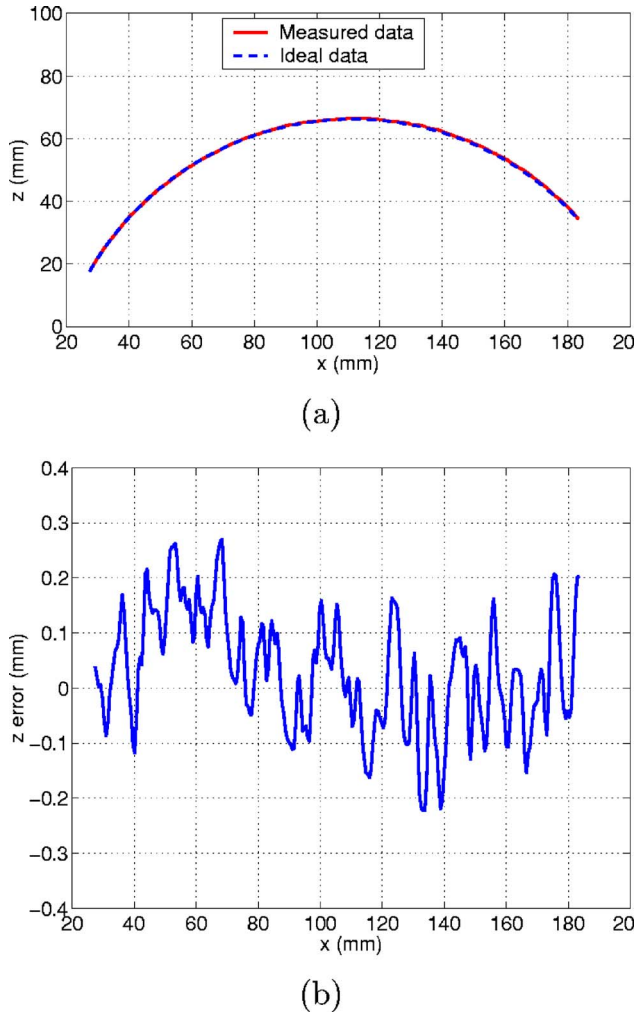

Fig. 12 Measurement result of a cylindrical surface: (a) cross section of the measured shape and (b) shape error.

The purpose of system calibration is to find the relationships between the camera coordinate system and the world coordinate system, and also the projector coordinate system and the same world coordinate system. These relationships can be expressed as

$$\boldsymbol{X}^c = \boldsymbol{M}^c \boldsymbol{X}^w,$$

$$\boldsymbol{X}^p = \boldsymbol{M}^p \boldsymbol{X}^w,$$

where $\boldsymbol{M}^c = [R^c, t^c]$ is the transformation matrix between the camera coordinate system and the world coordinate system, $\boldsymbol{M}^p = [R^p, t^p]$ is the transformation matrix between the projector coordinate system and the world coordinate system, and $\boldsymbol{X}^c = \{x^c, y^c, z^c\}^T$, $\boldsymbol{X}^p = \{x^p, y^p, z^p\}^T$, and $\boldsymbol{X}^w = \{x^w, y^w, z^w, 1\}^T$ are the coordinate matrices for point p (see Fig. 8) in the camera, projector, and the world coordinate systems, respectively. $\boldsymbol{X}^c$ and $\boldsymbol{X}^p$ can be further transformed to their CCD and DMD image coordinates (u^c, v^c) and (u^p, v^p) by applying the intrinsic matrices $\boldsymbol{A}^c$ and $\boldsymbol{A}^p$, because the intrinsic parameters are already calibrated. That is,

$$s^c\{u^c, v^c, 1\}^T = \boldsymbol{A}^c \boldsymbol{X}^c,$$

$$s^p\{u^p, v^p, 1\}^T = \boldsymbol{A}^p \boldsymbol{X}^p.$$

The extrinsic parameters can be obtained by the same procedures as those for the intrinsic parameters estimation. The only difference is that only one calibration image is needed to obtain the extrinsic parameters. The same Matlab toolbox provided by Bouguet[16] was utilized to obtain the extrinsic parameters. Example extrinsic parameter matrices for the system setup are

$$\boldsymbol{M}^c = \begin{bmatrix} 0.0163 & 0.9997 & -0.0161 & -103.4354 \\ 0.9993 & -0.0158 & 0.0325 & -108.1951 \\ 0.0322 & -0.0166 & -0.9993 & 1493.0794 \end{bmatrix},$$

$$\boldsymbol{M}^p = \begin{bmatrix} 0.0197 & 0.9996 & -0.0192 & -82.0873 \\ 0.9916 & -0.0171 & 0.1281 & 131.5616 \\ 0.1277 & -0.0216 & -0.9915 & 1514.1642 \end{bmatrix}.$$

2.5 *Phase-to-Coordinate Conversion*

Real measured object coordinates can be obtained based on the calibrated intrinsic and extrinsic parameters of the camera and the projector. Three phase-shifted fringe images and a centerline image are used to reconstruct the geometry of the surface. In the following, we discuss how to solve for the coordinates based on these four images.

For each arbitrary point (u^c, v^c) on the CCD image plane, its absolute phase can be calculated based on four images. This phase value can then be used to identify a line in the DMD image, which has the same absolute phase value. Without loss of generality, the line is assumed to be a vertical line with $u^p = \zeta[\phi_a(u^c, v^c)]$. Assuming world coordinates of the point to be (x^w, y^w, z^w), we have the following equation that transforms the world coordinates to the camera image coordinates:

$$s\{u^c, v^c, 1\}^T = \boldsymbol{P}^c\{x^w, y^w, z^w, 1\}^T, \tag{8}$$

where $\boldsymbol{P}^c = \boldsymbol{A}^c \boldsymbol{M}^c$ is the calibrated matrix for the camera. Similarly, we have the coordinate transformation equation for the projector,

$$s\{u^p, v^p, 1\}^T = \boldsymbol{P}^p\{x^w, y^w, z^w, 1\}^T, \tag{9}$$

where $\boldsymbol{P}^p = \boldsymbol{A}^p \boldsymbol{M}^p$ is the calibrated matrix for the projector. From Eqs. (8) and (9), we can obtain three linear equations,

$$f_1(x^w, y^w, z^w, u^c) = 0, \tag{10}$$

$$f_2(x^w, y^w, z^w, v^c) = 0, \tag{11}$$

$$f_3(x^w, y^w, z^w, u^p) = 0, \tag{12}$$

where u^c, v^c, and u^p are known. Therefore, the world coordinates (x^w, y^w, z^w) of the point p can be uniquely solved for the image point (u^c, v^c).

Downloaded From: http://opticalengineering.spiedigitallibrary.org/ on 11/05/2014 Terms of Use: http://spiedl.org/terms

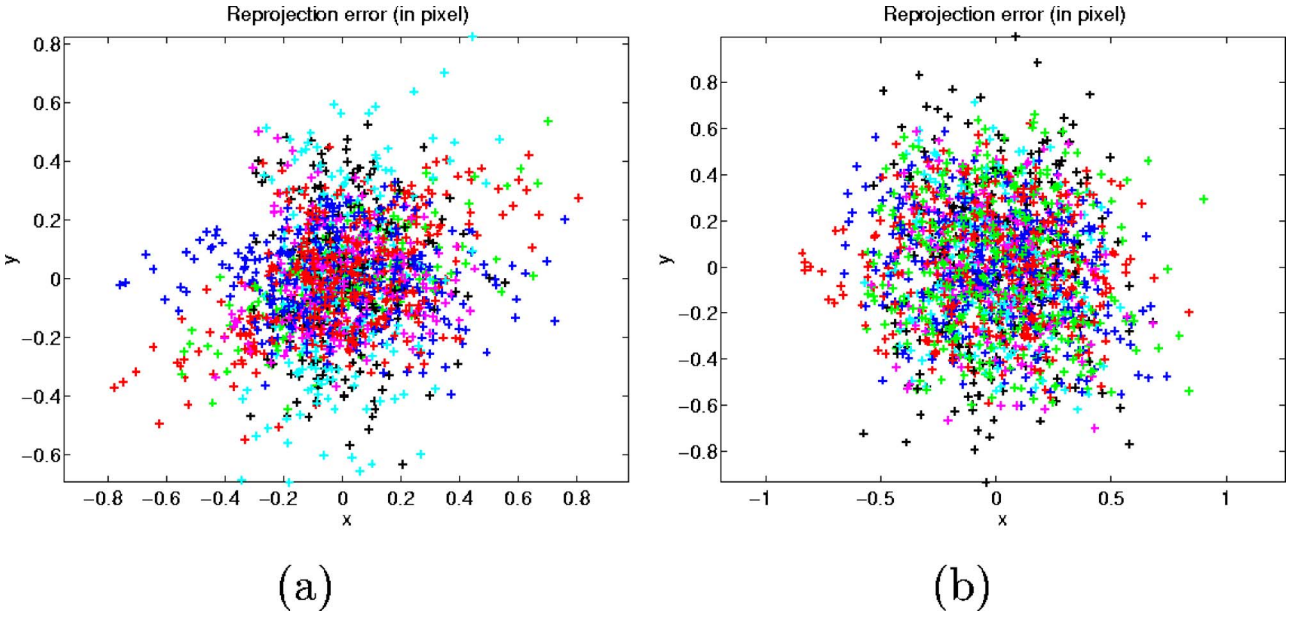

Fig. 13 Error caused by nonlinear image distortions: (a) error for the camera and (b) error for the projector.

3 Experiments

To verify the calibration procedures introduced in this research, we measured a planar board with a white surface using our system.[18] The measurement result is shown in Fig. 9(a). To determine the measurement error, we fit the measured coordinates with an ideal flat plane and calculate the distances between the measured points and the ideal plane. From the result, which is shown in Fig. 9(b), we found that the measurement error is less than rms 0.12 mm. In addition, we measured a sculpture Zeus, and the result is shown in Fig. 10. The first image is the object with texture mapping, the second image is the 3-D model of the sculpture in shaded mode, and the last one is the zoom-in view of the 3-D model. The reconstructed 3-D model is very smooth with details.

4 Calibration Evaluation

For more rigorous evaluation of this calibration method, we measured the same planar white board at 12 different positions and orientations. The results are shown in Fig. 11. The whole measurement volume is approximately 342(H) $\times$376(V)$\times$658(D) mm. The normals, x,y,z ranges, and the corresponding errors of the plane for each pose are listed in Table 1. We found that the error of the calibration method, which varies from rms 0.10 to 0.22 mm, did not depend on the orientation of the measured plane. We also found that the error was larger when the measured plane is far away from the system. We believe that this is primarily due to the fact that the images for our calibration were taken with the checkerboard located relatively close to the system. Therefore, for large volume measurement, calibration needs to be performed in the same volume to assure better accuracy.

To further verify that our calibration method is not significantly affected by the surface normal direction, we measured a cylindrical surface with a diameter of 200 mm. Figure 12 shows the measurement results. The error between the measured shape and the ideal one is less than rms 0.10 mm. These results demonstrate that the calibration is robust and accurate over a large volume.

5 Discussions

The calibration method proposed in this research for structured light systems has the following advantages over other methods

- *Simple*. The proposed calibration method separates the projector and camera calibration, which makes the calibration simple.
- *Simultaneous*. For each checkerboard calibration pose, the camera image and the projector image can be obtained simultaneously. Therefore, the camera and the projector can be calibrated simultaneously.
- *Fast*. The calibration of the projector and the camera follows the same procedures of camera calibration. A checkerboard can be utilized to calibrate the camera and the projector simultaneously. This is much faster than other calibration methods, in which complex optimization procedures often have to be involved to obtain the relationship between the camera and projector parameters.
- *Accurate*. Since the projector and camera calibrations are independent, there is no coupling issue involved, and thus more accurate parameters of the camera and projector can be obtained.

For the system we developed, we did not use the nonlinear model for the camera or the projector. Our experiments showed that the nonlinear model generated worse results. This is probably because the nonlinear distortion of the lenses used in our system is small, and the use of the nonlinear model might have caused numerical instability.[19,20] To verify that the nonlinear distortions of the

Downloaded From: http://opticalengineering.spiedigitallibrary.org/ on 11/05/2014 Terms of Use: http://spiedl.org/terms

camera and the projector are indeed negligible, we compute the errors of the corner points of the checkerboard at the image planes of the camera and projector, assuming a linear model. Here the error is defined as the difference between the coordinates of a checker corner point as computed from the real captured image and from the back projected image based on a linear model. Figure 13 shows the results. The errors for both the camera and projector are within ±1 pixel. Therefore, the linear model is sufficient to describe the camera and the projector of our system.

6 Conclusions

We introduce a novel calibration method for structured light systems that use projectors. The key concept is to treat the projector as a camera, and calibrate the camera and the projector independently using the traditional calibration method for cameras. To allow the projector to be treated as a camera, we develop a new method that enables the projector to "capture" images like a camera. With this new concept, the calibration of structured light systems becomes essentially the same as that of traditional stereovision systems, which is well established. This calibration method is implemented and tested in our structured light system. The maximum calibration error is found to be rms 0.22 mm over a volume of $342(\mathrm{H}) \times 376(\mathrm{V}) \times 658(\mathrm{D})$ mm. The calibration method is fast, robust, and accurate. It significantly simplifies the calibration and recalibration procedures of structured light systems. In addition to applications in calibration, the concept of enabling a projector to "capture" images may also have potential other applications in computer graphics, medical imaging, plastic surgery, etc.

Acknowledgments

This work was supported by the National Science Foundation under grant number CMS-9900337 and National Institute of Health under grant number RR13995.

References

1. R. Legarda-Sáenz, T. Bothe, and W. P. Jüptner, "Accurate procedure for the calibration of a structured light system," *Opt. Eng.*, **43**(2), 464–471 (2004).
2. F. J. Cuevas, M. Servin, and R. Rodriguez-Vera, "Depth object recovery using radial basis functions," *Opt. Commun.* **163**(4), 270–277 (1999).
3. F. J. Cuevas, M. Servin, O. N. Stavroudis, and R. Rodriguez-Vera, "Multi-layer neural networks applied to phase and depth recovery from fringe patterns," *Opt. Commun.* **181**(4), 239–259 (2000).
4. C. C. Slama, C. Theurer, and S. W. Henriksen, *Manual of Photogrammetry*, 4th ed., Am. Soc. of Photogram., Falls Church, VA (1980).
5. C. S. Fraser, "Photogrammetric camera component calibration: A review of analytical techniques," in *Calibration and Orientation of Camera in Computer Vision*, A. Gruen and T. S. Huang, Eds., pp. 95–136, Springer-Verlag, Berlin, Heidelberg (2001).
6. A. Gruen and H. A. Beyer, "System calibration through self-calibration," in *Calibration and Orientation of Camera in Computer Vision*, A. Gruen and T. S. Huang, Eds., pp. 163–194, Springer-Verlag, Berlin, Heidelberg (2001).
7. J. Heikkilä, "Geometric camera calibration using circular control," *IEEE Trans. Pattern Anal. Mach. Intell.* **22**(10), 1066–1077 (2000).
8. F. Pedersini, A. Sarti, and S. Tubaro, "Accurate and simple geometric calibration of multi-camera systems," *Signal Process.* **77**(3), 309–334 (1999).
9. D. B. Gennery, "Least-square camera calibration including lens distortion and automatic editing of calibration points," in *Calibration and Orientation of Camera in Computer Vision*, A. Gruen and T. S. Huang, Eds., pp. 123–136, Springer-Verlag, Berlin, Heidelberg (2001).
10. Q. Hu, P. S. Huang, Q. Fu, and F. P. Chiang, "Calibration of a 3-d shape measurement system," *Opt. Eng.* **42**(2), 487–493 (2003).
11. D. C. Brown, "Close-range camera calibration," *Photogramm. Eng.* **37**(8), 855–866 (1971).
12. W. Faig, "Calibration of close-range photogrammetry system: Mathematical formulation," *Photogramm. Eng. Remote Sens.* **41**(12), 1479–1486 (1975).
13. C. Slama, *Manual of Photogram.*, 4th ed., American Society of Photogrammetry, Falls Church, VA (1980).
14. J. Weng, P. Cohen, and M. Herniou, "Camera calibration with distortion models and accuracy evaluation," *IEEE Trans. Pattern Anal. Mach. Intell.* **14**(10), 965–980 (1992).
15. Z. Zhang, "A flexible new technique for camera calibration," *IEEE Trans. Pattern Anal. Mach. Intell.* **22**(11), 1330–1334 (2000).
16. J. Y. Bouguet, "Camera calibration toolbox for matlab," see http://www.vision.caltech.edu/bouguetj/calib_doc.
17. D. C. Ghiglia and M. D. Pritt, *Two-Dimensional Phase Unwrapping: Theory, Algorithms, and Software*, John Wiley and Sons, New York (1998).
18. S. Zhang and P. Huang, "High-resolution, real-time 3-d shape acquisition," *IEEE Computer Vision Patt. Recog. Workshop (CVPRW'04)* **3**(3), 28–37 (2004).
19. R. Y. Tsai, "A versatile camera calibration technique for high-accuracy 3d machine vision metrology using off-the-shelf tv camera and lenses," *IEEE J. Rob. Autom.* **3**(4), 323–344 (1987).
20. G. Wei and S. Ma, "Implicit and explicit camera calibration: Theory and experiments," *IEEE Trans. Pattern Anal. Mach. Intell.* **16**(5), 469–480 (1994).

Song Zhang is a post-doctoral fellow at Harvard University. He obtained his BS degree from the University of Science and Technology of China in 2000, and his MS and PhD degrees the mechanical engineering department of the State University of New York at Stony Brook, in 2003 and 2005, respectively. His research interests include optical metrology, 3-D machine and computer vision, human computer interaction, image processing, computer graphics, etc.

Peisen S. Huang obtained his BS degree in precision instrumentation engineering from Shanghai Jiao Tong University, China, in 1984, his ME and DrEng degrees in precision engineering and mechatronics from Tohoku University, Japan, in 1988 and 1995, respectively, and his PhD degree in mechanical engineering from The University of Michigan, Ann Arbor, in 1993. He has been a faculty member in the Department of Mechanical Engineering, Stony Brook University, since 1993. His research interests include optical metrology, image processing, 3-D computer vision, etc.

Downloaded From: http://opticalengineering.spiedigitallibrary.org/ on 11/05/2014 Terms of Use: http://spiedl.org/terms